Catalysis of Thiol Oxidation by Cobalamins and Cobinamides: Reaction Products and Kinetics†

Donald W. Jacobsen,* Lawrence S. Troxell, and Kenneth L. Brown

ABSTRACT: The corrinoid coenzymes adenosylcobalamin and methylcobalamin and their cobinamide analogues adenosylcobinamide and methylcobinamide catalyzed the aerobic oxidation of 2-mercaptoethanol and dithioerythritol in a dark-reaction model system. The rates of these reactions were directly proportional to catalyst concentration and were generally maximal at slightly alkaline pH. The pseudo-first-order rate constants for the catalysis of 2-mercaptoethanol oxidation at pH 8.0 by alkylcobinamides and aquacobalamin, which are aquated at *single* axial-ligand positions, were as follows: methylaquacobinamide, 0.19 s^{-1}; adenosylaquacobinamide, 0.17 s^{-1}; aquacobalamin, 0.17 s^{-1}. Diaquacobinamide, which is aquated at *both* axial-ligand positions, catalyzed the same reaction 1000 times faster (k_1 = 190 s^{-1}). In contrast, alkylcobalamins that contain sterically inaccessible or blocked axial-ligand positions catalyzed thiol oxidation slowly (k_1 = 0.003 and 0.004 s^{-1} for methylcobalamin and adenosylcobalamin, respectively). The pseudo-first-order rate constants for corrinoid catalysis of dithioerythritol oxidation followed the same pattern except that the values were generally 2–3 times higher. The products of aerobic dithioerythritol oxidation were hydrogen peroxide and the cyclic disulfide of dithioerythritol. They accumulated stoichiometrically as demonstrated by a predictable release of oxygen after addition of catalase and by spectrophotometric observation of cyclic disulfide formation. Enthalpies of activation for the catalysis of 2-mercaptoethanol oxidation at pH 8.0 by aquacobalamin, adenosylcobalamin, diaquacobinamide, adenosylaquacobinamide, and methylaquacobinamide were 15.5, 16.6, 17.2, 17.7, and 18.8 kcal mol^{-1}, respectively, whereas the corresponding entropies of activation were 17.5, 14.1, 35.4, 24.9, and 28.8 eu, respectively.

An event common to most if not all of the corrinoid-dependent enzyme systems is cleavage of the carbon–cobalt bond of the coenzyme participating in the reaction. For example, the corrinoid-dependent methyltransferases catalyze reactions that necessitate the making and breaking of carbon–cobalt bonds of methylcobalamin (Me-Cbl)[1] (Taylor &Weissbach, 1973). In addition, there is good evidence that adenosylcobalamin- (Ado-Cbl) dependent enzyme systems catalyze substrate–product transformations by processes requiring coenzyme scission (Babior, 1975; Abeles & Dolphin, 1976; Krouwer & Babior, 1977). The mechanism of coenzyme activation that results in the cleavage of the carbon–cobalt bond is unknown. Studies from several laboratories have suggested that enzyme sulfhydryl groups may be important functional entities in corrinoid-dependent catalysis. Thus, the apoenzyme forms of diol dehydrase (Lee & Abeles, 1963) and methylmalonyl-CoA mutase (Cannata et al., 1965) are sensitive to *p*-(hydroxymercuri)benzoate and other sulfhydryl group reagents whereas the holoenzymes that contain Ado-Cbl are protected from inactivation by these compounds. Moreover, several corrinoid-dependent enzyme systems contain subunits that have been characterized as "thiol proteins" and that are essential for activity. Examples include glutamate mutase (Switzer & Barker, 1967), L-β-lysine mutase (Stadtman & Renz, 1968), D-α-lysine mutase (Morley & Stadtman, 1970), and glycerol dehydrase (Schneider et al., 1970). Toraya et al. (1974) reported that diol dehydrase contained a protein subunit with sulfhydryl groups, and Kuno et al. (1981) have attempted to establish which of these are essential for enzyme activity. Corrinoid-dependent ribonucleotide reductases interact directly with dithiol substrates (e.g., thioredoxin, dihydrolipoate, or dithioerythritol) in order to catalyze the formation of 2′-deoxyribonucleotides (Hogenkamp & Sando, 1974). Vitols et al. (1967) reported that the external dithiol substrate activated the apoenzyme by reduction of a disulfide bond. Of no less importance is the role played by reducing substrates, including mono- and dithiols, in the conversion of the vitamin cyanocobalamin (CN-Cbl) to its coenzyme forms Ado-Cbl and Me-Cbl (Huennekens, 1968).

In an attempt to elucidate the role of enzyme sulfhydryl groups in cobalamin-dependent catalysis, a detailed study on the interactions of corrinoids with thiols and dithiols has been conducted in this laboratory. This paper describes and extends work on the general properties of corrinoid-dependent thiol oxidation (Peel, 1962, 1963; Aronovitch & Grossowicz, 1962; Schrauzer & Sibert, 1969; Agnes et al., 1971; Frick et al., 1976) and specifically deals with the aerobic oxidation of 2-mercaptoethanol (ME) and dithioerythritol (DTE) catalyzed by Ado-Cbl, adenosylaquacobinamide (Ado-Cbi), aquacobalamin (Aq-Cbl), and diaquacobinamide [$(Aq)_2$-Cbi]. The results of selected studies with CN-Cbl, Me-Cbl, methylaquacobinamide (Me-Cbi), and cyanoaquacobinamide (CN-Cbi) are also included in this paper.

Experimental Procedures

Materials. The following items were obtained from commercial sources: catalase (types CTR and CTS, Worthington); CN-Cbl, L-cysteine, EDTA, dithioerythritol, and DL-α-lipoic

† From the Division of Biochemistry, Department of Basic and Clinical Research, The Research Institute of Scripps Clinic, La Jolla, California 92037, and the Department of Chemistry, University of Texas at Arlington, Arlington, Texas 76019. *Received June 8, 1983.* This work was supported by Grants AM25406 and CA6522 from the National Institutes of Health and Grant Y-749 from the Robert A. Welch Foundation, Houston, TX. This is Publication No. 2948-BCR from The Research Institute of Scripps Clinic.

[1] Abbreviations: Me-Cbl, methylcob(III)alamin; CN-Cbl, cyanocob(III)alamin (vitamin B_{12}); Ado-Cbl, adenosylcob(III)alamin (B_{12} coenzyme); Aq-Cbl, aquacob(III)alamin (vitamin B_{12a}); Ado-Cbi, adenosylaquacob(III)inamide; Me-Cbi, methylaquacob(III)inamide; CN-Cbi, cyanoaquacob(III)inamide; $(Aq)_2$-Cbi, diaquacob(III)inamide; ME, 2-mercaptoethanol; DTE, dithioerythritol; DTE_{ox}, *cis*-4,5-dihydroxy-*o*-dithiane (cyclic disulfide of DTE); DTNB, 5,5′-dithiobis(2-nitrobenzoic acid); EDTA, ethylenediaminetetraacetic acid; HPLC, high-pressure liquid chromatography.

0006-2960/84/0423-2017$01.50/0

acid (Sigma); 2-mercaptoethanol (Eastman; distilled under argon in vacuo before use); phosphocellulose (Bio-Rad). The following buffers (0.2 ionic strength) were used in this study: glycine hydrochloride (pH 2–3); sodium acetate (pH 4–5); sodium potassium phosphate (pH 6–7.8); Trizma-HCl (pH 7.6–8.6); sodium bicarbonate–carbonate (pH 9.0–11.0) (Long, 1961). Other buffers included 0.5 M sodium phosphate (pH 11–13), 0.5 M (cyclohexylamino)propanesulfonic acid (CAPS; pH 9.0–10.5), and 2-[[tris(hydroxymethyl)methyl]amino]-ethanesulfonic acid (TES; pH 7–8). All buffers contained 1.0×10^{-3} M EDTA.

Dihydrolipoic acid was prepared by the method of Gunsalus & Razzell (1957) except that the product was titrated under argon with 5 N NaOH to pH 7.0. The yield of sodium dihydrolipoate, on the basis of DTNB analysis (see below), was 98%. Aq-Cbl and CN-Cbi, synthesized from CN-Cbl by the procedures of Hogenkamp & Rush (1968) and Friedrich & Bernhauer (1956), respectively, were purified by ion-exchange chromatography on phosphocellulose. $(Aq)_2$-Cbi was prepared from either Aq-Cbl by hydrolysis (Pailes & Hogenkamp, 1968) or CN-Cbi by catalytic hydrogenation (Hogenkamp & Rush, 1968). Alkylcorrinoids were synthesized, purified, and tested under dim-red illumination to avoid photolysis. Ado-Cbl was synthesized by the method of Jacobsen et al. (1975) and repurified immediately before use to remove traces of CN-Cbl and Aq-Cbl as follows. A total of 50 mg of crystalline Ado-Cbl was dissolved in 5 mL of water and applied to phosphocellulose (2.5×30 cm column) that had been washed successively with 1.0 M KCl and water until free of chloride. Ado-Cbl was eluted from the column with water, concentrated by evaporation in vacuo (35 °C), and recrystallized from aqueous acetone at 4 °C. Me-Cbl was synthesized by a modification of the procedure of Wood et al. (1968) as described previously (Jacobsen et al., 1975). Ado-Cbi and Me-Cbi were synthesized from CN-Cbi and 5′-chloroadenosine and methyl bromide (Jacobsen et al., 1975), respectively. The compounds were repurified immediately before use by chromatography on phosphocellulose.

Methods. The purity of corrinoids was ascertained from electronic absorption spectra and by thin-layer chromatography on cellulose and silica gel (Firth et al., 1968), paper electrophoresis (Volcani et al., 1961), and by HPLC (Jacobsen et al., 1982). The concentration of corrinoids was determined spectrophotometrically after conversion to their dicyano form (367 nm, $a_M = 3.04 \times 10^4$ M^{-1} cm^{-1}; Pratt, 1972). Thiols were determined by the method of Ellman (1959), slightly modified as follows. A total of 0.8 mL of DTNB reagent, prepared fresh by diluting 0.2 mL of stock DTNB (4 mg/mL in ethanol) to 25 mL with 0.5 M Trizma-HCl (pH 8.0), was mixed with 0.2 mL of aqueous thiol. After 5 min at room temperature, the absorbance at 412 nm ($a_M = 1.36 \times 10^4$ M^{-1} cm^{-1}) was determined. Thiols in reaction mixes were determined by withdrawing 5–10 μL from the polarographic cell and by injecting it directly into the DTNB reagent.

The rate of oxygen disappearance during corrinoid catalysis of thiol oxidation was measured polarographically as described by Peel (1962, 1963) except that a Gilson Oxygraph (Model KM) equipped with a Clark oxygen electrode was used to monitor changes in the concentration of dissolved O_2. The electrode cell was maintained to within ± 0.2 °C of the desired operating temperature by a thermostatically controlled circulating water bath. The oxygen electrode was calibrated with air-saturated distilled water. After the cell had reached thermal equilibrium (25 °C), the recorder of the polarograph was set to full scale (180 mm), corresponding to 2.58×10^{-4} M O_2, the concentration of O_2 in air-saturated water at 25 °C (Washburn, 1928). The base line (i.e., O_2 concentration = 0) was established by adding a few milligrams of sodium dithionite to the polarographic cell. Oxygen uptake during corrinoid catalysis of thiol oxidation was determined as follows. Air-saturated buffer (1.40 mL) was added to the polarographic cell and allowed to reach thermal equilibrium. Thiol substrates in deoxygenated water (0.20 mL) were then added to the cell, which resulted in an O_2 dilution and rapid pen deflection (ca. 14%). After the background rate of thiol oxidation (k_b) was established, corrinoids in 25 μL of aqueous solution were injected through the capillary port into the cell. The rate of O_2 consumption (k) was again determined after waiting a few seconds for the system to reach steady state. The net rate of O_2 consumption (k_0) due to corrinoid-dependent catalysis was obtained by difference ($k_0 = k - k_b$).

The rate of cyclic disulfide formation during the oxidation of DTE and dihydrolipoate was followed in a Cary 14 recording spectrophotometer equipped with a 0–0.1 absorbance unit slide wire as follows. The base line of the recorder was adjusted to zero absorbance with reference and sample cuvettes containing identical concentrations of air-saturated buffer and dithiol. If absorbance (283 and 333 nm for DTE and dihydrolipoate, respectively) remained constant, it was assumed that the reference and sample cuvettes had identical background rates of autooxidation. Corrinoids were then injected into the sample cuvette to initiate catalysis of dithiol oxidation. The rate and extent of cyclic disulfide formation was calculated from the change in absorbance at 283 ($a_M = 2.73 \times 10^2$ M^{-1} cm^{-1}) or 333 nm ($a_M = 1.33 \times 10^2$ M^{-1} cm^{-1}). The acid dissociation constants of DTE were determined at 25 °C by the method of Zahler & Cleland (1968).

Hydrogen peroxide, which accumulated during corrinoid-dependent thiol oxidation, was determined polarographically by adding catalase (1000 units in 25 μL of aqueous solution) to the reaction cell after approximately 50% of the dissolved O_2 had been consumed. A rapid increase in O_2 concentration on the polarographic trace indicated that accumulated hydrogen peroxide had undergone immediate decomposition in the presence of the added catalase. In some experiments, catalase was added to the reaction prior to the addition of corrinoid to prevent accumulation of hydrogen peroxide during the course of thiol oxidation.

Alkylcorrinoids were photolyzed by illuminating the polarographic cell with a high-intensity lamp (Tensor Model 4975) positioned 3 cm from the center of the vessel. Circulating water from a constant-temperature bath (25 ± 0.2 °C) surrounded the reaction cell and prevented heat buildup during the photolysis period (10–60 s).

Results

Kinetics of Oxygen Uptake. Corrinoids promoted the rapid utilization of dissolved O_2 during the catalysis of thiol oxidation as shown in Figure 1. In this representative experiment, the rate of O_2 consumption reached steady state shortly after the addition of catalyst, and it remained linear until O_2 concentrations dropped below 50 μM. The zero-order rate constant (k_0) for O_2 uptake was calculated from the linear portion of the profile ($k_0 = k - k_b$). The pseudo-first-order rate constant (k_1) was determined from the concentration of the catalyst in the reaction ($k_1 = k_0/M_{Cbl}$). Most corrinoids including Ado-Cbl, Me-Cbl, CN-Cbi, and $(Aq)_2$-Cbi generated the type of profile shown in Figure 1, irrespective of wide variations in experimental parameters such as pH, temperature, and substrate and catalyst concentration. However, significant lag periods were observed (up to 70 s; data not shown) when

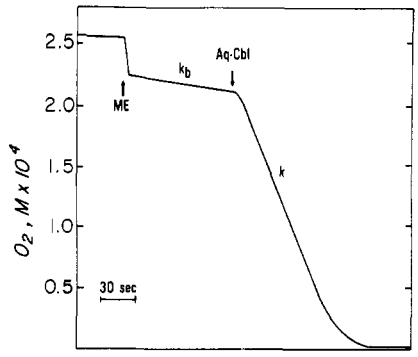

FIGURE 1: Polarographic measurement of oxygen uptake during the catalysis of ME oxidation by Aq-Cbl. The order of additions to the polarographic cell was as follows: 1.40 mL of 0.34 M Trizma-HCl (pH 8.0) containing 0.001 M EDTA; 0.20 mL of 0.20 M ME; 0.025 mL of 6.5 × 10^{-4} M Aq-Cbl. The addition of thiol substrate (anaerobic) caused an immediate pen deflection (ca. 14%) due to the dilution of dissolved O_2. Temperature was 25 ± 0.2 °C.

Table I: Pseudo-First-Order Rate Constants for O_2 Disappearance and DTE_{ox} Formation[a]

catalyst	O_2 disappearance, k_1 (s^{-1})[b]	DTE_{ox} formation, k_1 (s^{-1})[c]	ratio O_2/DTE_{ox}
Aq-Cbl	0.57 ± 0.03	0.63 ± 0.04	0.91
Ado-Cbi	0.49 ± 0.03	0.46 ± 0.05	1.07
$(Aq)_2$-Cbi	567 ± 28	597 ± 36	0.95

[a] Initial substrate [DTE] = 1.25 × 10^{-2} M; pH 8.0. [b] The rate of O_2 disappearance was determined polarographically at 25 ± 0.2 °C as described under Methods. [c] The rate of DTE_{ox} formation was determined spectrophotometrically at 26 ± 2 °C as described under Methods.

CN-Cbl served as a catalyst for ME oxidation before the rate of O_2 consumption became linear. Two other corrinoids, Ado-Cbi and Me-Cbi, generated slightly atypical profiles of O_2 uptake, particularly in the presence of dithiol substrates. Thus, the rate of O_2 consumption accelerated slowly during the catalysis of DTE oxidation by Me-Cbi and Ado-Cbi (data not shown). This phenomenon, which appeared to be autocatalytic in nature, was not observed if catalase was included in the reaction. These results suggested that hydrogen peroxide was a reaction product and may have been responsible for the slow conversion of Ado-Cbi and Me-Cbi into more active catalysts.

Formation of Hydrogen Peroxide. Hydrogen peroxide accumulated during the course of corrinoid-catalyzed thiol oxidation as demonstrated by the addition of catalase to the system (Figure 2). This resulted in an abrupt increase in O_2 concentration during the course of Aq-Cbl-catalyzed ME oxidation (Figure 2A) and amounted to approximately 50% of the O_2 previously consumed (when extrapolated back to the time of catalase injection). The rate of O_2 uptake in the presence of catalase was only half of the value observed in its absence. Similar results were obtained for the oxidation of ME catalyzed by Ado-Cbi (Figure 2B) and by $(Aq)_2$-Cbi (data not shown). Addition of heat-denatured enzyme had no effect on O_2 concentration or disappearance rate.

Formation of Cyclic Disulfide. The formation of the cyclic disulfide of DTE (DTE_{ox}) during catalysis of its oxidation by Aq-Cbl, $(Aq)_2$-Cbi, and Ado-Cbi was followed spectrophotometrically. The rate of formation of DTE_{ox} was nearly identical with the rate of O_2 disappearance as shown in Table I. The stoichiometry of O_2 consumption and DTE_{ox} formation was 1:1 between pH 7 and 8. Similar results were obtained for the catalysis of sodium dihydrolipoate oxidation by Aq-Cbl

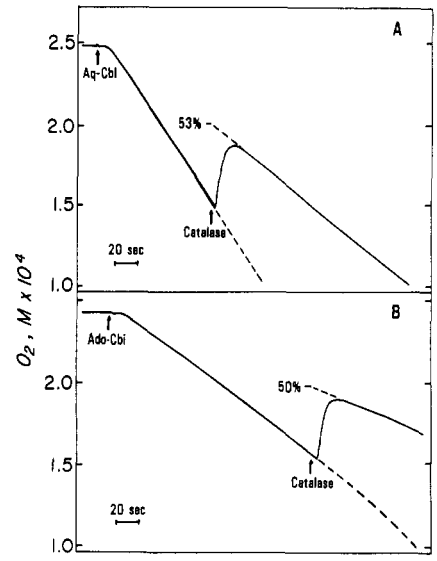

FIGURE 2: Effect of catalase on the rate of O_2 utilization during ME oxidation catalyzed by Aq-Cbl (A) and Ado-Cbi (B). The order of additions to the polarographic cell was as follows: 1.40 mL of sodium–potassium phosphate (P_i = 0.088 M, pH 7.0) containing 0.001 M EDTA; 0.20 mL of 0.20 M ME; corrinoid [0.025 mL of 5.0 × 10^{-4} M Aq-Cbl in (A) and 0.025 mL of 3.9 × 10^{-4} M Ado-Cbi in (B)]; 0.025 mL of an aqueous solution of catalase (975 units). Addition of catalase resulted in a rapid increase in O_2 concentrtion (approximately 50% of that previously consumed when extrapolated back to the time of enzyme addition). In (A), k_0 was 1.06 × 10^{-6} M O_2 s^{-1} before catalase addition and 5.69 × 10^{-7} M O_2 s^{-1} after its addition. In (B), the values were 5.46 × 10^{-7} M O_2 s^{-1} and 3.00 × 10^{-7} M O_2 s^{-1}, respectively. Temperature was 25 ± 0.2 °C.

and $(Aq)_2$-Cbi when cyclic lipoate formation was followed spectrophotometrically at 333 nm. The oxidation of thiols by hydrogen peroxide (Slater, 1952), which was observed after O_2 depletion, occurred at a much slower rate.

Effect of Corrinoid Concentration on Reaction Rates. The rate of O_2 uptake during the catalysis of ME oxidation at pH 8.0 by $(Aq)_2$-Cbi, Aq-Cbl, and Ado-Cbi was directly proportional to corrinoid concentration (data not shown). Similar results have been reported by Peel (1963) for the aerobic oxidation of ME catalyzed by CN-Cbi, CN-Cbl, and Aq-Cbl and by Schrauzer & Sibert (1969) for corrinoid catalysis of methylene blue reduction by ME.

Thiol Concentration. The effect of increasing thiol concentration on the rate of O_2 consumption was dependent upon the individual corrinoid catalyzing the reaction as shown in Figure 3. Increasing ME concentration appeared to saturate the $(Aq)_2$-Cbi-catalyzed reaction (Figure 3A) with a half-maximal velocity (apparent K_m) observed at 0.08 M while DTE appeared to saturate with an apparent K_m of 0.045 M (Figure 3B). In the case of Ado-Cbi-dependent catalysis, ME appeared to saturate at lower concentrations (K_m = 0.024 M) as shown in Figure 3C. At higher thiol concentrations (i.e., 0.2 M), the rates of O_2 uptake increased beyond that predicted from saturation kinetics, which suggested that, under these conditions, Ado-Cbi was converted into a more active catalytic form. Deviation from saturation kinetics was more readily apparent for Me-Cbi as shown in Figure 3D. Finally, the rate of O_2 uptake during catalysis of ME oxidation by Aq-Cbl did not exhibit saturation behavior (Figure 3E) at higher thiol concentrations.

Hydrogen Ion Concentration. The effects of pH on the rates of O_2 uptake during corrinoid catalysis of ME and DTE oxidation are shown in Figure 4. A well-defined rate maximum occurred at pH 8.9 for the catalysis of ME oxidation by Ado-Cbi (Figure 4A). The low catalytic activity of Ado-Cbl

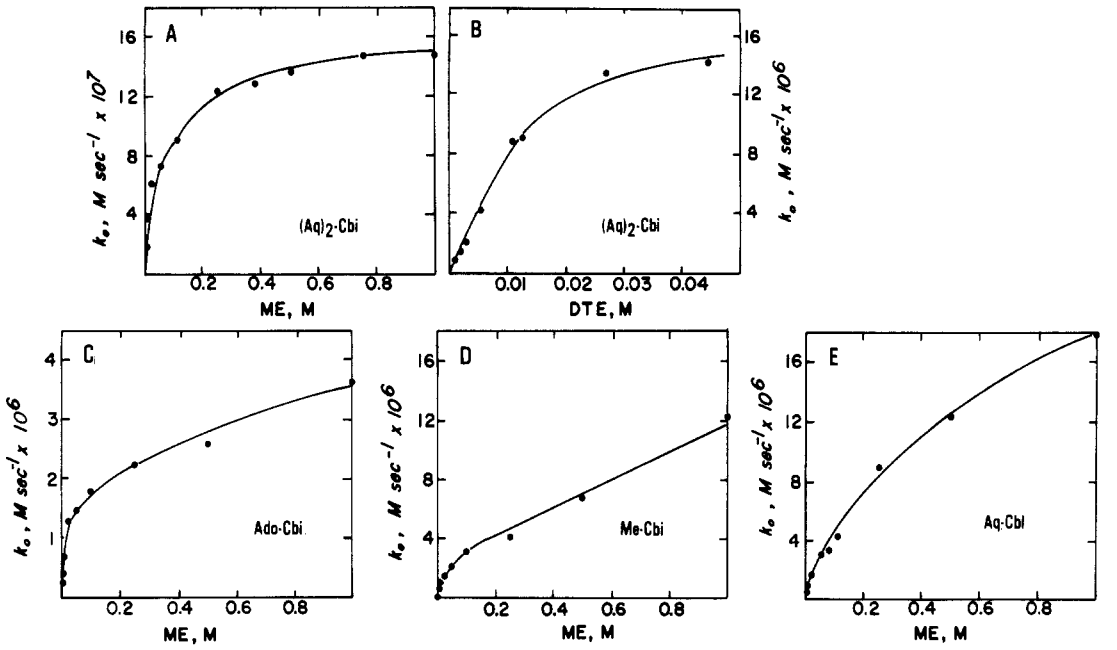

FIGURE 3: Dependence of the rate of O_2 uptake on thiol concentration. The reaction mixtures contained 0.30 M Trizma chloride (pH 8.0), 8.70×10^{-4} M EDTA, thiol as indicated, and 5.00×10^{-9} M $(Aq)_2$-Cbi (A), 1.87×10^{-8} M $(Aq)_2$-Cbi (B), 6.00×10^{-6} M Ado-Cbi (C), 6.47×10^{-6} M Me-Cbi (D), or 1.10×10^{-5} M Aq-Cbl (E). Temperature was 25 ± 0.2 °C.

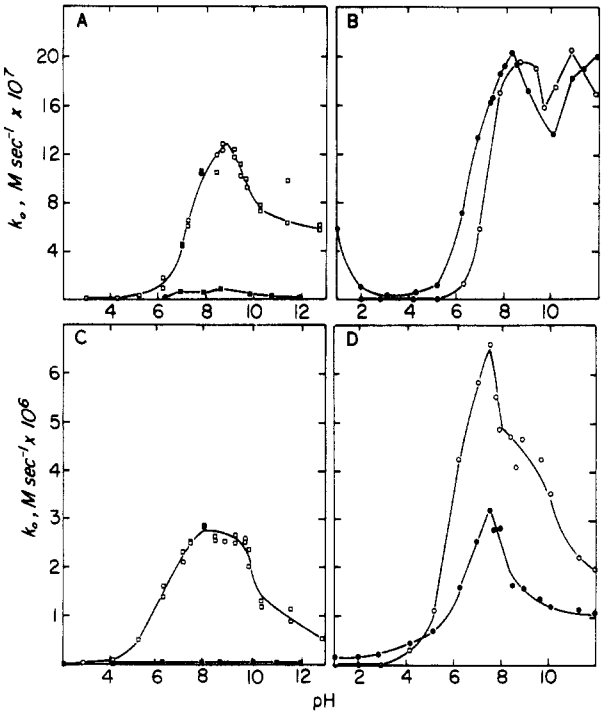

FIGURE 4: Effect of hydrogen ion concentration on the rate of O_2 uptake during corrinoid-dependent catalysis of ME oxidation (A and B) and DTE oxidation (C and D). Reaction mixtures in (A) and (B) contained buffers at the indicated pH (see Methods for buffer composition), 8.7×10^{-4} M EDTA, 0.025 M ME, and 2.66×10^{-5} M Ado-Cbl (■), 6.00×10^{-6} M Ado-Cbi (□), 1.13×10^{-5} M Aq-Cbl (●), or 9.25×10^{-9} M $(Aq)_2$-Cbi (○) in a final volume of 1.63 mL. Reaction mixtures in (C) and (D) contained buffers at the indicated pH, 8.7×10^{-4} M EDTA, 0.0125 M DTE, and 1.82×10^{-5} M Ado-Cbl (■), 6.00×10^{-6} M Ado-Cbi (□), 5.00×10^{-6} M Aq-Cbl (●), or 9.10×10^{-9} M $(Aq)_2$-Cbi (○) in a final volume of 1.63 mL. Temperature was 25 ± 0.20 °C.

toward ME oxidation precluded a definite assignment of a pH maximum although activity could be detected over the range 6–12 (Figure 4A). Well-defined rate maxima occurred at pH 8.4 and 8.7 for the catalysis of ME oxidation by Aq-Cbl and $(Aq)_2$-Cbi, respectively (Figure 4B). $(Aq)_2$-Cbi had a second optimum in the alkaline range at pH 10.9 but was inactive below pH 5.0. In contrast, Aq-Cbl not only had high activity up to pH 13 but also was significantly active at pH 1.0.

Table II: Effect of Light on Pseudo-First-Order Rate Constants for Catalysis of ME Oxidation at pH 8

catalyst	k_1 (s^{-1}) dark reaction	k_1 (s^{-1}) after photolysis[a]
Ado-Cbl	0.004	0.102 (20 s)
Me-Cbl	0.003	0.184 (20 s)
CN-Cbl	0.080	0.080 (60 s)
Aq-Cbl	0.167	0.167 (20 s)
Ado-Cbi	0.172	177.0 (60 s)
Me-Cbi	0.192	122.0 (90 s)
CN-Cbi	175.0	175.0 (30 s)
$(Aq)_2$-Cbi	190.0	190.0 (60 s)

[a] The dark reaction pseudo-first-order rate constant was established as described under Methods. Midway during the course of the reaction, the polarographic cell was exposed to high-intensity light from a tungsten-filament source for the time indicated in parentheses. A lag time (usually less than 10 s) preceeded the establishment of the new rate for those reactions demonstrating photosensitivity. Reaction temperature was 25 ± 0.2 °C before and after photolysis. The concentration of ME was 0.025 M.

A broad pH optimum was observed for the catalysis of DTE oxidation by Ado-Cbi, which extended from 7.5 to 9.6 (Figure 4C). In contrast, Ado-Cbl-dependent catalysis of DTE oxidation was barely detectable between pH 5 and 12 even though the catalyst concentration was relatively high. The catalysis of DTE oxidation was characterized by sharp pH maxima at 7.5 for $(Aq)_2$-Cbi and Aq-Cbl as shown in Figure 4D. The latter catalyst was again active at pH 1.0.

Me-Cbi and CN-Cbi did not catalyze ME oxidation below pH 5.0, but above pH 6, rate profiles similar to those of $(Aq)_2$-Cbi (Figure 4B) and Ado-Cbi (Figure 4A), respectively, were observed (data not shown). Thus, the rates for Me-Cbi catalysis continued to increase up to pH 13, while the rates for CN-Cbi had a well-defined maximum at around pH 9.0.

Light. The photodecomposition of *alkyl*cobalamins and *alkyl*cobinamides during the course of thiol oxidation resulted in enhanced rates of O_2 consumption (Table II). After a 20-s

Table III: Activation Parameters for Corrinoid-Catalyzed Oxidation of ME

catalyst	$\Delta H^{\ddagger}$ (kcal mol^{-1})	$\Delta S^{\ddagger}$ (eu)
Ado-Cbl	16.55 ± 1.40	14.09 ± 4.63
Me-Cbi	18.77 ± 0.20	28.77 ± 0.65
Aq-Cbl	15.53 ± 0.38	17.49 ± 1.26
Ado-Cbi	17.71 ± 0.59	24.90 ± 1.93
$(Aq)_2$-Cbi	17.18 ± 0.25	35.44 ± 0.81

exposure of the polarographic cell to a high-intensity tungsten-filament lamp during Ado-Cbl- or Me-Cbl-catalyzed ME oxidation, a 50-fold rate increase occurred that was similar to the rate observed with Aq-Cbl. When photolysis was allowed to occur during ME oxidation catalyzed by Ado-Cbi and Me-Cbi, the rate of O_2 consumption increased over 1000- and 635-fold, respectively. Light had no effect on catalysis of ME oxidation by CN-Cbl, Aq-Cbl, CN-Cbi, and $(Aq)_2$-Cbi (Table II).

Temperature. The rates of O_2 uptake during the catalysis of ME oxidation of Aq-Cbl, Ado-Cbl, $(Aq)_2$-Cbi, Ado-Cbi, and Me-Cbi were determined between the temperatures of 10 and 50 °C. As shown in Figure 5, linear relationships were obtained by plotting ln $[kh/(k_BT)]$ vs. $1/T$. The entropies ($\Delta S^{\ddagger}$) and enthalpies ($\Delta H^{\ddagger}$) of activation for the reactions are summarized in Table III.

Discussion

The early findings of Peel (1962, 1963) that corrinoids catalyze the oxidation of thiol have been extended by the current study to encompass a variety of cobalamin and cobinamide analogues. Polarographic methods were used to follow the disappearance of O_2 during the course of these reactions. The rate of O_2 disappearance during corrinoid-catalyzed thiol oxidation was constant until depletion (see Figure 1), suggesting that the reaction was zero order with respect to the concentration of the terminal electron acceptor. Peel (1963) also found that O_2 uptake was constant during the catalysis of ME oxidation by CN-Cbi, Aq-Cbl, and CN-Cbl, and Schrauzer & Sibert (1969) noted a zero-order dependence on the concentration of methylene blue during the anaerobic catalysis of ME oxidation by the same three corrinoids. In the latter study, methylene blue replaced O_2 as the terminal electron acceptor.

In this study, the products of aerobic thiol oxidation that were formed during the corrinoid-catalyzed reaction have been identified as hydrogen peroxide and the corresponding disulfide. The former product was indirectly demonstrated by injecting catalase into the polarographic cell midway during the course of the reaction, which resulted in an abrupt increase in O_2 concentration and a resumption of O_2 disappearance at 50% of the original rate (Figure 2). These observations are consistent with (1) the conversion O_2 to hydrogen peroxide according to reaction 1, (2) the return of 50% of the O_2 to the system according to reaction 2 in the presence of catalase, and (3) a net result that produces a 50% decrease in O_2 disappearance rate (reaction 3).

$$2RSH + O_2 \xrightarrow{Cbl} RSSR + H_2O_2 \quad (1)$$

$$H_2O_2 \xrightarrow{catalase} {}^1/_2O_2 + H_2O \quad (2)$$

$$2RSH + {}^1/_2O_2 \xrightarrow[catalase]{Cbl} RSSR + H_2O \quad (3)$$

The formation of cyclic disulfides was observed spectrophotometrically during corrinoid-catalyzed oxidation of DTE and dihydrolipoate. The rate and extent of cyclic disulfide

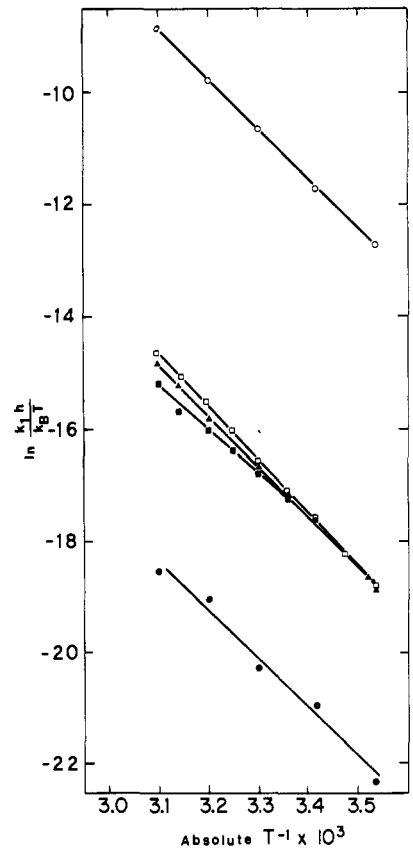

FIGURE 5: Effect of temperature on the pseudo-first-order rate constant for the catalysis of ME oxidation by $(Aq)_2$-Cbi (○), Me-Cbi (□), Ado-Cbi (▲), Aq-Cbl (■), and Ado-Cbl (●). Trizma-HCl at a final concentration of 0.30 M (pH 8.0 at 25 °C) and containing 8.7×10^{-4} M EDTA was the buffer used for reaction catalyzed by Ado-Cbl (2.54×10^{-5} M), Aq-Cbl (1.00×10^{-5} M), and Ado-Cbi (6.00×10^{-6} M). TES–HCl at a final concentration of 0.25 M (pH 8.0 at 25 °C) and containing 8.7×10^{-4} M EDTA was used for the reactions catalyzed by Me-Cbi (7.78×10^{-6} M) and $(Aq)_2$-Cbi (4.65×10^{-9} M). The final concentration of ME was 0.025 M. The changes in pH accompanying temperature changes were determined experimentally for the two buffer systems. This was necessary in order to correct small but significant changes in the rate of O_2 uptake as a function of pH. Oxygen solubility in water at different temperatures was calculated from the *International Critical Tables* (Washburn, 1928). The data are plotted according to transition-state theory.

formation equaled the rate and extent of O_2 uptake (Table I) for DTE oxidation catalyzed by Ado-Cbi, $(Aq)_2$-Cbi, and Aq-Cbl. The stoichiometries for dithiol oxidation (reaction 4) and for monothiol oxidation (reaction 1) are in agreement

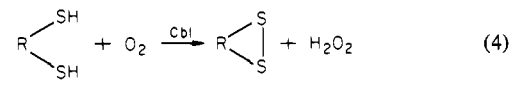

(4)

with the stoichiometry observed by Schrauzer & Sibert (1969) for corrinoid-catalyzed reduction of methylene blue to leukomethylene blue by thiols. Cystine and homocystine were identified by Aronovitch & Grossowicz (1962) as the corrinoid-catalyzed aerobic oxidation products of cysteine and homocysteine, respectively. The fact that earlier studies involving corrinoid-catalyzed thiol oxidation (Aronovitch & Grossowicz, 1962; Peel, 1963) failed to identify hydrogen peroxide as the other initial product of these reactions may have been due to secondary reactions involving the oxidation of thiols by hydrogen peroxide (Slater, 1952). Hydrogen peroxide has been identified as the primary product of aerobic thiol oxidation catalyzed by copper ion (Slater, 1952; De Marco et al., 1971), other metal ions (Capozzi and Modena, 1974), and cobalt–dithiolene complex (Dance et al., 1974).

The rate of O_2 disappearance during corrinoid-catalyzed thiol oxidation was dependent upon both catalyst and thiol concentration. The zero-order rate constants (k_0) were directly proportional to corrinoid concentration. The effect of thiol concentration on k_0 was somewhat variable depending upon the corrinoid (see Figure 3). For $(Aq)_2$-Cbi and Ado-Cbi, saturation behavior was observed as the ME concentration increased. Peel (1963) observed saturation behavior for the catalysis of ME oxidation by CN-Cbi and reported an apparent K_m of 0.03 M. Deviation from saturation behavior was observed with Me-Cbi and most notably with Aq-Cbl.

Visible light had a pronounced stimulatory effect on the rates of O_2 disappearance during the catalysis of ME oxidation by alkylcobalamins (Ado-Cbl, Me-Cbl) and alkylcobinamides (Ado-Cbi, Me-Cbi) but had no effect on the reactions catalyzed by Aq-Cbl, CN-Cbi, and $(Aq)_2$-Cbi (see Table II). Thus, photolysis of the carbon–cobalt bond of the former compounds resulted in the formation of more active catalysts, e.g.

$$\text{Ado-Cbl} \xrightarrow{h\nu} \text{Aq-Cbl} \qquad \text{Ado-Cbi} \xrightarrow{h\nu} (Aq)_2\text{-Cbi}$$

Formulation of a general mechanism for corrinoid-catalyzed thiol oxidation required a detailed investigation on the effects of hydrogen ion and hydroxyl ion concentration on the kinetics of O_2 uptake. During preliminary studies, it was readily apparent that background rates of thiol oxidation at alkaline pH (particularly with the dithiol substrate dihydrolipoic acid) would mask the rates of the corrinoid-dependent reactions. For this reason, background rates of thiol oxidation were largely suppressed by adding EDTA to all reaction buffers at a final concentration of 1.0 mM, thereby allowing rate measurements to be made over a broad pH range.

Although the effects of hydrogen ion concentration on the rates of O_2 uptake were complex (see Figure 4), a general pattern of reactivity, based predominately on the acid dissociation constants of the thiol substrates (Crampton, 1974), emerges from these data. Distinct rate maxima were observed between pH 8 and 9 when ME was the substrate, and since its reported pK_a is 9.43 at 25 °C (Kreevoy et al., 1960), there appears to be a dependency upon the concentrations of both thiol (RSH) and thiolate anion (RS^-). Brown & Kallen (1972) have shown that thiols (RSH) displace water from methylaquocobaloxime at a much faster rate than thiolate anions (RS^-). Thus, the initial complexation of thiol to corrinoids is likely to proceed at a faster rate at lower pHs.

The dissociation constants of DTE, determined in this laboratory at 25 °C, were 9.06 (pK_1) and 9.96 (pK_2). The pH–rate profiles of DTE oxidation (Figure 4C,D) indicate maxima between 7.5 and 8.5, again suggesting that a thiol and thiolate anion may be involved in the reaction mechanism. The observation that both the ME and DTE pH–rate profiles are shifted below their primary pK_a values by approximately 1.3–1.4 pH units would seem to indicate a slightly more important role for the thiol group. Alternatively, the formation of corrinoid–thiol complexes, particularly in the case of the dithiol substrate, could significantly lower the apparent pK_a of thiol by inductive effects (Hanania & Irvine, 1964).

Proton dissociations from aquated corrinoids, as observed for the conversion of Aq-Cbl to HO-Cbl (reaction 5) with a

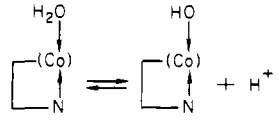

(5)

reported pK_a of 7.72–7.80 (Hanania & Irvine, 1964; Hayward et al., 1965), may also play a role in catalytic activity. Thus, axial-ligand exchange rates are influenced to some extent by the nature of the leaving group (i.e., H_2O or HO^-) as described by Randall & Alberty (1966). Further support for this has been provided by Brown et al. (1972, 1975), who observed that equilibrium constants for displacement of HO^- from alkylhydroxocobaloximes by added ligands were substantially lower than those for displacement of H_2O from the same alkylaquocobaloximes by the same added ligands.

On the basis of the above observations and considerations, the following reactions may explain the mechanism of corrinoid-catalyzed thiol oxidation:

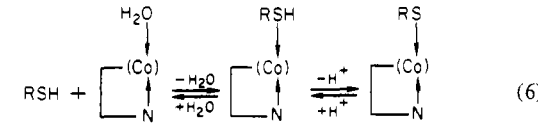

(6)

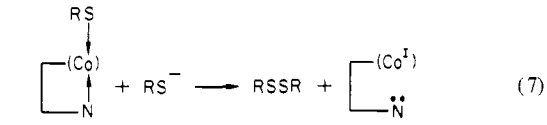

(7)

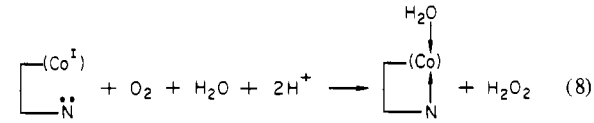

(8)

In reaction 6, a complex is formed between the thiol and the corrinoid at the axial-ligand position of the latter. Proton loss probably occurs concomitant with or subsequent to complex formation, resulting in the formation of a coordinate bond between cobalt and sulfur. The complex formed between glutathione and Aq-Cbl, which is reasonably stable and can be isolated, has a characteristic UV–vis absorbance spectrum (Dubnoff, 1964). Similar spectra for complexes formed between Aq-Cbl and L-cysteine, DTE, and dihydrolipoic acid are shown in Figure 6. Because of their lability, the dithiol–Cbl complexes were observed at low temperature between pH 5 and 7. However, even under similar conditions, it has not been possible to observe the ME-Cbl complex, which must be much more labile.

The corrinoid–thiol complex undergoes nucleophilic attack by thiolate anion to form a reduced corrinoid and the disulfide (reaction 7). Thiolate anion comes from a second substrate molecule during ME oxidation but, in the case of DTE oxidation, is contained within the corrinoid–dithiol complex. The final step in the mechanism (reaction 8) is the regeneration of the reduced corrinoid catalyst by molecular oxygen. Evidence for a two-electron-reduced corrinoid intermediate will be presented elsewhere (D. W. Jacobsen et al., unpublished results).

Formulation of a rate law, which is in agreement with the general mechanism given by reactions 6–8, and the assumption that reaction 7 is the rate-determining step, leads to the following expression:

$$k_1 = k_f k_{rds} K_a K_{RSH}[H^+][RSH]_T^2/(K_a k_{rds} K_{RSH}^2[RSH]_T + [(k_f + k_{rds})K_a K_{RSH}[RSH]_T + k_r K_{RSH}^2][H^+] + [(K_a + K_{RSH})k_f[RSH]_T + 2k_r K_{RSH}][H^+]^2 + (k_f[RSH]_T + k_r)[H^+]^3)$$

In this derivation, the rate constants k_f and k_r were assigned to the forward and reverse reactions of the first step of reaction 6. The proton transfer in the second step of reaction 6 was assumed to be rapid and was assigned the acid dissociation constant K_a. Reaction 7 was assumed to be the rate-determining step with a rate constant k_{rds} and a pK_a of the thiol K_{RSH}. A steady-state assumption was made of the thiol–

Table IV: Comparison of Pseudo-First-Order Rate Constants for Corrinoid-Catalyzed Oxidation of ME and DTE[a]

		ME		DTE	
group	catalyst	k_1 (s^{-1})	pH	k_1 (s^{-1})	pH
I	Ado-Cbl	0.003 ± 0.001	broad	0.001 ± 0.0005	broad
	Me-Cbl	0.003 ± 0.001	7.0[b]	ND[c]	
II	CN-Cbl	0.080 ± 0.004	8.0[b]	ND	
	Aq-Cbl	0.180 ± 0.009	8.4	0.64 ± 0.03	7.5
	Ado-Cbi	0.230 ± 0.012	8.9	0.46 ± 0.02	7.5–9.5
	Me-Cbi	0.560 ± 0.028	11–13	ND	
III	CN-Cbi	191 ± 10	8.5–9.5	ND	
	$(Aq)_2$-Cbi	211 ± 11	8.8	725 ± 36	7.5

[a] Pseudo-first-order rate constants were calculated from pH–rate profiles and represent rate maxima at the indicated pH or pH range. [b] Measurement was made at the indicated pH only. [c] ND = not determined.

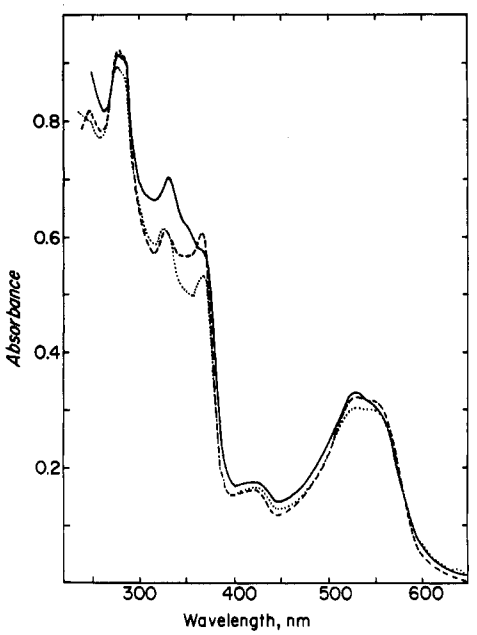

FIGURE 6: Formation of mono- and dithiol complexes with Aq-Cbl. The L-cysteine–Cbl complex (– –) was formed at 0 °C by adding 25 μmol of L-cysteine (in 0.5 mL of water) to 40 nmol of Aq-Cbl in 0.5 mL of 0.76 M sodium acetate, pH 4.25, containing 0.001 M EDTA. The DTE–Cbl complex (···) was formed at 0 °C by adding 25 μmol of DTE (in 0.5 mL of water) to 40 nmol of Aq-Cbl in 0.5 mL of 0.76 M sodium acetate, pH 4.25, containing 0.001 M EDTA. The dihydrolipoic acid–Cbl complex (—) was formed at 0 °C by adding 25 μmol of dihydrolipoic acid (in 0.5 mL of water) to 40 nmol of Aq-Cbl in 0.5 mL of 0.088 M sodium–potassium phosphate, pH 7.0, containing 0.001 M EDTA. Spectra were recorded at 0 °C in a Cary 14 spectrophotometer.

corrinoid complex. At sufficiently high thiol concentration, the rate law collapses to a form that is first order in thiol:

$$\lim_{[RSH]_T \to \infty} k_1 = k_f k_{rds} K_a K_{RSH} [H^+][RSH]_T / (K_a k_{rds} K_{RSH}^2 + (k_f + k_{rds}) K_a K_{RSH} [H^+] + (K_a + K_{RSH}) k_f [H^+]^2 + k_f [H^+]^3)$$

i.e., at a given pH

$$\lim_{[RSH]_T \to \infty} k_1 = \text{constant} \times [RSH]$$

This is precisely the behavior (at given pH) shown by the data in Figure 3. Reaction 8 was assumed to be fast and not rate limiting; however, in order to determine whether the rate-limiting step is reaction 6 or 7, additional studies will be required. Preliminary experiments suggest that the rate-limiting step involves thiolate anion attack on the corrinoid–thiol complex (reaction 7).

The activity of corrinoids as catalysts of thiol oxidation span nearly 6 orders of magnitude as shown in Table IV. The alkylcobalamins (Ado-Cbl and Me-Cbl) are weak catalysts and yield reaction rates that are just detectable by the polarographic method. The possibility that a contaminant such as Aq-Cbl or $(Aq)_2$-Cbi might be responsible for the observed low catalytic activity was considered unlikely for the following reasons: (1) Me-Cbl and Ado-Cbl were synthesized and purified to homogeneity as judged by spectral analysis, thin-layer chromatography, and HPLC; (2) the derived pseudo-first-order rate constants for purified material from different syntheses were always comparable; (3) repeated purification of Ado-Cbl on phosphocellulose did not diminish its low but significant catalytic activity.

The alkylcobinamides (Ado-Cbi and Me-Cbi) and the cobalamin Aq-Cbl comprise a second class of catalysts with intermediate activity (group II, Table IV). Pseudo-first-order rate constants (k_1) vary from 0.18 for Aq-Cbl to 0.56 for Me-Cbi during the catalysis of ME oxidation and are approximately 2–3 times higher when DTE is the substrate. The observation that alkylcobinamides are active catalysts of thiol oxidation has important mechanistic implications. For this reason, these compounds have been subjected to rigid and repeated purifications to eliminate the possibility of contamination by Aq-Cbl or $(Aq)_2$-Cbi.

The most active class of corrinoid catalysts of thiol oxidation are the cobinamides, which do not have a covalent ligand at either axial position (group III, Table IV). Thus, $(Aq)_2$-Cbi and CN-Cbi catalyze ME oxidation at rates several orders of magnitude higher than the cobalamins or alkylcobinamides. The rate of DTE oxidation catalyzed by $(Aq)_2$-Cbi is again about 3 times higher than the rate of ME oxidation.

The critical factors that determine corrinoid catalytic activity appear to be the number of exposed axial-ligand positions and their accessibility to undergo ligand exchange reactions. The alkylcobalamins of group I in Table IV, which contain a covalently attached group as the upper axial ligand and a bulky nucleotide coordinated to the lower axial position, are poor catalysts of thiol oxidation. The low but detectable activity of Ado-Cbl and Me-Cbl can be explained by the fact that the lower axial ligand equilibrates between "base-on" and "base-off" conformations (Hayward et al., 1965), exposing the lower axial position to solvent or solute. In the base-off conformation, alkylcobalamins such as Ado-Cbl and Me-Cbl resemble alkylcobinamides. The equilibria for this process are shown in reaction 9, where $K_{Bz} = [II][H^+][I]^{-1}$ and $K_{Co} =$

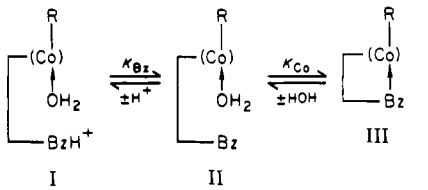

(9)

Table V: Estimation of Percent Base-Off Forms of Me-Cbl and Ado-Cbl and Correlation with the Relative Catalytic Activity of the Analogous Cbi Forms

R-Cbl	pK_a	K_{Co}	% base-off	$k_{R\text{-}Cbl}/k_{R\text{-}Cbi} \times 100$ (pH 8)	$k_{R\text{-}Cbl}/k_{R\text{-}Cbi} \times 100$ (pH_{max})
Me-Cbl	2.72	94.5	1.05	1.56	0.53
Ado-Cbl	3.35	21.4	4.46	2.33	1.30

$[III][II]^{-1}$. The overall, apparent pK_a, $K_a = ([II] + [III])[H^+][I]^{-1}$, is given by $K_a = (1 + K_{Co})K_{Bz}^{-1}$. If pK_{Bz} is assumed to be the reported pK_a of 1-β-D-ribo-5,6-dimethylbenzimidazole, i.e., 4.70 (Davies et al., 1951), then K_{Co} can be calculated for Me-Cbl and Ado-Cbl from their reported pK_a values of 2.72 and 3.35, respectively (Hogenkamp et al., 1965; Hayward et al., 1965). This allows for an estimate of the percentages of base-on and base-off forms of R-Cbl at slightly basic pHs as shown in Table V. The last two columns in this table are the ratios [expressed in percent of the catalytic constants (k_1)] for R-Cbl and R-Cbi at pH 8.0 (from Table II) and at the pH maxima (from Table IV) for the reactions. Although the comparisons are not exact, it is clear that the decrease in catalytic efficiency in going from R-Cbi to the analogous R-Cbl is reasonably well accounted for by the ratio of base-on to base-off species for R-Cbl. The mechanism for the catalysis of monothiol oxidation by Ado-Cbl is shown in reactions 10 and 11. Reoxidation of reduced Ado-Cbl would

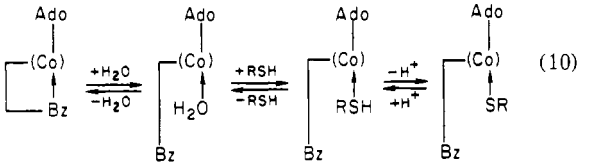

(10)

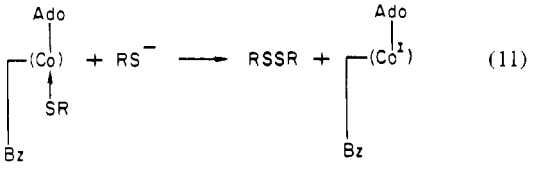

(11)

proceed as in reaction 8. The observation that the rate of DTE oxidation catalyzed by Ado-Cbl is actually lower than the rate of ME oxidation (see Table III) probably reflects a steric hinderance problem associated with the larger dithiol substrate.

The corrinoids in group II have either a single axial-ligand position exposed to solvent molecules (viz., Aq-Cbl, Ado-Cbi, and Me-Cbi) or a coordinated axial ligand (viz., CN-Cbl) that readily undergoes exchange reactions with other nucleophiles. The rates of DTE oxidation are significantly higher than the rates of ME oxidation due to the lack of a steric hinderance problem and the intramolecular association of the second thiol (or thiolate anion) group. The corrinoids in group III (Table IV), the most active catalysts of thiol oxidation, have both axial-ligand positions exposed for interaction with solvent or solute molecules. The presence of a noncovalently coordinated cyanide group in CN-Cbi only slightly diminishes the catalytic activity of this cobinamide, and it is quite possible that the CN^- group is rapidly displaced in the presence of thiols. The high catalytic activity of cobinamides, partially explained by the availability of two complex formation sites, might also result from the association of O_2 with the complex prior to thiolate anion attack (reaction 12).

The activation parameters determined for five of the catalytic reactions and summarized in Table III lend support to

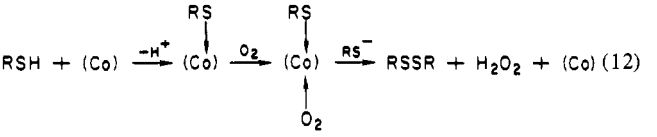

(12)

the idea that the mechanisms for each of the reactions may be similar. The fact that there is little variation in $\Delta H^\ddagger$ (mean $\Delta H^\ddagger = 17.15 \pm 1.22$) implies that the bond-making and bond-breaking processes in the transition states are similar for the five catalysts (e.g., RSH coordination to Co may dominate the enthalpy of activation and occurs to about the same extent for all five transition states). Essentially all of the differences in rates are due to differences in $\Delta S^\ddagger$. The latter are large and positive, implying that the loss of freedom of motion due to the coordination of RSH is more than compensated for by the increased freedom of motion as a result of the loss of the leaving ligand. This might explain why Ado-Cbl has the lowest $\Delta S^\ddagger$ since displacement of the pendant nucleotide would not increase entropy as much as complete loss of a coordinated H_2O (i.e., as in Me-Cbi, Aq-Cbl, and Ado-Cbi). The very high $\Delta S^\ddagger$ for $(Aq)_2$-Cbi implies that both coordinated H_2O molecules are lost during catalysis of thiol oxidation.

Finally, Costa and his co-workers have synthesized and characterized a series of corrinoid model compounds (Costa, 1972) that closely mimic the redox properties of cobalamins (Elliott et al., 1981). One of these compounds R-Co[C_2-(D)$(DOH)_{pn}$], which contains an axial carbon–cobalt bond, can undergo a two-electron reduction to the Co(I) oxidation state without cleavage of the C–Co bond (Costa et al., 1971). Another closely related complex, Me-Co[$(tn)H_2O$]$^+$, can react with thiols to form trans-axial thiol complexes and can catalyze aerobic thiol oxidation without cleavage of the Me–Co bond (Pellizer et al., 1973).

In summary, our studies demonstrate that thiols readily interact with corrinoids and that the reactivity is dependent upon the nature of axial ligation. The interactions involve thiol–corrinoid complexation and electron-transfer reactions. Although these studies do not attempt to explain how corrinoid coenzymes function enzymatically, they do suggest that enzyme sulfhydryl groups or substrate thiols could interact successfully with the coenzyme forms, perhaps as a first step in the activation of the carbon–cobalt bond. Intracellular thiols may also participate as reducing substrates in the biosynthetic conversion of the vitamin to its coenzyme forms. Thus, in the presence of a donor group substrate (e.g., *S*-adenosylmethionine), the reduced corrinoid produced in reaction 7 might undergo alkylation to give a coenzyme form (e.g., Me-Cbl).

Acknowledgments

We are greatly indebted to Dr. F. M. Huennekens for his helpful advice and encouragement. Expert technical assistance was provided by Sharon Murphy-Jackson and Yolanda Montejano. We also thank Karin Vitols for assisting in the preparation of the manuscript.

Registry No. Ado-Cbl, 13870-90-1; Me-Cbl, 13422-55-4; CN-Cbl, 68-19-9; Aq-Cbl, 13422-52-1; Ado-Cbi, 89302-86-3; Me-Cbi, 15653-35-7; CN-Cbi, 13963-62-7; $(Aq)_2$-Cbi, 15259-55-9; ME, 60-24-2; DTE, 6892-68-8; DTE_{ox}, 40227-25-6; dihydrolipoic acid, 462-20-4.

References

Abeles, R. H., & Dolphin, D. (1976) *Acc. Chem. Res. 9*, 114–120.

Agnes, G., Hill, H. A. O., Pratt, J. M., Ridsdale, S. C., Kennedy, F. S., & Williams, R. J. P. (1971) *Biochim. Biophys. Acta 252*, 207–211.

Aronovitch, J., & Grossowicz, N. (1962) *Biochem. Biophys. Res. Commun. 8*, 416–420.

Babior, B. M. (1975) in *Cobalamin* (Babior, B. M., Ed.) pp 141–212, Wiley-Interscience, New York.

Brown, K. L., & Kallen, R. G. (1972) *J. Am. Chem. Soc. 94*, 1894–1901.

Brown, K. L., Chernoff, K., Keljo, D. J., & Kallen, R. G. (1972) *J. Am. Chem. Soc. 94*, 6697–6704.

Brown, K. L., Lyles, D., Pencovici, M., & Kallen, R. G. (1975) *J. Am. Chem. Soc. 97*, 7338–7346.

Cannata, J. J. B., Focesi, A., Mazuder, R., Warner, R. C., & Ochoa, S. (1965) *J. Biol. Chem. 240*, 3249–3257.

Capozzi, G., & Modena, G. (1974) in *The Chemistry of the Thiol Group* (Patai, S., Ed.) Part 2, pp 806–824, Wiley-Interscience, New York.

Costa, G. (1972) *Coord. Chem. Rev. 8*, 63–75.

Costa, G., Puxeddu, A., & Reisenhofer, E. (1971) *J. Chem. Soc., Chem. Commun.*, 993–994.

Crampton, M. R. (1974) in *The Chemistry of the Thiol Group* (Patai, S., Ed.) Part 1, pp 379–415, Wiley-Interscience, New York.

Dance, I. G., Conrad, R. C., & Cline, J. E. (1974) *J. Chem. Soc., Chem. Commun.*, 13–14.

Davies, M. T., Mamalis, P., Petrow, V., & Sturgeon, B. (1951) *J. Pharm. Pharmacol. 3*, 420–430.

De Marco, C., Dupre, S., Crifo, C., Rotillo, G., & Cavallini, D. (1971) *Arch. Biochem. Biophys. 144*, 496–502.

Dubnoff, J. W. (1964) *Biochem. Biophys. Res. Commun. 16*, 484–488.

Elliot, C. M., Hershenhart, E., Finke, R. G., & Smith, B. L. (1981) *J. Am. Chem. Soc. 103*, 5558–5566.

Ellman, G. L. (1959) *Arch. Biochem. Biophys. 82*, 70–77.

Firth, R. A., Hill, H. A. O., Pratt, J. M., & Throp, R. G. (1968) *Anal. Biochem. 23*, 429–432.

Frick, T., Francia, M. D., & Wood, J. M. (1976) *Biochim. Biophys. Acta 428*, 808–818.

Friedrich, W., & Bernhauer, K. (1956) *Chem. Ber. 89*, 2507–2512.

Gunsalus, I. C., & Razzell, W. E. (1957) *Methods Enzymol. 3*, 941–946.

Hanania, G. I. H., & Irvine, D. H. (1964) *J. Chem. Soc.*, 5694–5697.

Hayward, G. C., Hill, H. A. O., Pratt, J. M., Vanston, N. J., & Williams, R. J. P. (1965) *J. Chem. Soc.*, 6485–6493.

Hogenkamp, H. P. C., & Rush, J. E. (1968) *Biochem. Prep. 12*, 121–124.

Hogenkamp, H. P. C., & Sando, G. N. (1974) *Struct. Bonding (Berlin) 20*, 23–58.

Hogenkamp, H. P. C., Rush, J. E., & Swenson, C. A. (1965) *J. Biol. Chem. 240*, 3641–3644.

Huennekens, F. M. (1968) in *Biological Oxidations* (Singer, S. T. P., Ed.) pp 439–523, Wiley-Interscience, New York.

Jacobsen, D. W., Di Girolamo, P. M., & Huennekens, F. M. (1975) *Mol. Pharmacol. 11*, 174–184.

Jacobsen, D. W., Green, R., Quadros, E. V., & Montejano, Y. D. (1982) *Anal. Biochem. 120*, 394–403.

Kreevoy, M. M., Harper, E. T., Duvall, R. E., Wilgus, H. S., & Ditsch, L. T. (1960) *J. Am. Chem. Soc. 82*, 4899–4902.

Krouwer, J. S., & Babior, B. M. (1977) *Mol. Cell. Biochem. 15*, 80–108.

Kuno, S., Toraya, T., & Fukui, S. (1981) *Arch. Biochem. Biophys. 210*, 474–480.

Lee, H. A., & Abeles, R. H. (1963) *J. Biol. Chem. 238*, 2367–2373.

Long, C., Ed. (1961) *Biochemist's Handbook*, pp 30–41, Van Nostrand, Princeton, NJ.

Morley, C. G. D., & Stadtman, T. C. (1970) *Biochemistry 9*, 4890–4900.

Pailes, W. H., & Hogenkamp, H. P. C. (1968) *Biochemistry 7*, 4160–4166.

Peel, J. L. (1962) *J. Biol. Chem. 237*, PC263–PC265.

Peel, J. L. (1963) *Biochem. J. 88*, 296–308.

Pellizer, G., Tauszik, G. R., & Costa, G. (1973) *J. Chem. Soc., Dalton Trans. 193*, 317–322.

Pratt, J. M. (1972) *Inorganic Chemistry of Vitamin B_{12}*, p 46, Academic Press, New York.

Randall, W. C., & Alberty, R. A. (1966) *Biochemistry 5*, 3189–3193.

Schneider, Z., Larsen, E. G., Jacobson, G., Johnson, B. C., & Paelkiewicz, J. (1970) *J. Biol. Chem. 245*, 3380–3396.

Schrauzer, G. N., & Sibert, J. (1969) *Arch. Biochem. Biophys. 130*, 257–266.

Slater, E. C. (1952) *Nature (London) 170*, 970–971.

Stadtman, T. C., & Renz, P. (1968) *Arch. Biochem. Biophys. 125*, 226–239.

Switzer, R. L., & Barker, H. A. (1967) *J. Biol. Chem. 242*, 2658–2674.

Taylor, R. T., & Weissbach, H. (1973) *Enzymes, 3rd Ed. 9*, 121–165.

Toraya, T., Weska, M., & Fukui, S. (1974) *Biochemistry 13*, 3895–3899.

Vitols, E., Hogenkamp, H. P. C., Brownson, C., Blakley, R. L., & Connellan, J. (1967) *Biochem. J. 104*, 58c–60c.

Volcani, B. E., Toohey, J. I., & Barker, H. A. (1961) *Arch. Biochem. Biophys. 92*, 381–391.

Washburn, E. W. (1928) *International Critical Tables*, Vol. III, p 258, McGraw-Hill, New York.

Wood, J. M., Kennedy, F. S., & Wolfe, R. S. (1968) *Biochemistry 7*, 1707–1713.

Zahler, W. L., & Cleland, W. W. (1968) *J. Biol. Chem. 243*, 716–719.